Article

Magnetically Responsive Carboxylated Magnetite-Polydipyrrole/ Polydicarbazole Nanocomposites of Core–Shell Morphology. Preparation, Characterization, and Use in DNA Hybridization

Jean-Paul Lellouche, Govindaraji Senthil, Augustine Joseph, Ludmila Buzhansky, Ian Bruce, Erika R. Bauminger, and Jacob Schlesinger

J. Am. Chem. Soc., **2005**, 127 (34), 11998-12006• DOI: 10.1021/ja050285l • Publication Date (Web): 10 August 2005

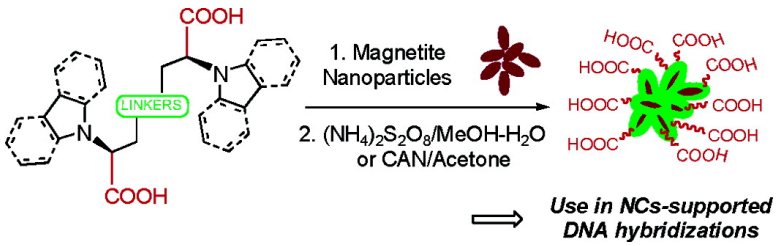

More About This Article

Additional resources and features associated with this article are available within the HTML version:

- Supporting Information
- Links to the 3 articles that cite this article, as of the time of this article download
- Access to high resolution figures
- Links to articles and content related to this article
- Copyright permission to reproduce figures and/or text from this article

View the Full Text HTML

J|A|C|S
ARTICLES
Published on Web 08/10/2005

Magnetically Responsive Carboxylated Magnetite-Polydipyrrole/Polydicarbazole Nanocomposites of Core−Shell Morphology. Preparation, Characterization, and Use in DNA Hybridization

Jean-Paul Lellouche,*,† Govindaraji Senthil,† Augustine Joseph,†
Ludmila Buzhansky,† Ian Bruce,‡ Erika R. Bauminger,§ and Jacob Schlesinger||

Contribution from the Department of Chemistry, Bar-Ilan University, Ramat-Gan 52900, Israel, Department of Biosciences, University of Kent, Canterbury, Kent, ME4 4TB, United Kingdom, Racah Institute of Physics, the Hebrew University, Jerusalem, Israel, and Savyon Diagnostics Ltd., 3 Habosem Street, Ashdod 77610, Israel

Received January 16, 2005; E-mail: lellouj@mail.biu.ac.il

Abstract: Novel bis-heterocyclic mono- and dicarboxylated dipyrrole and dicarbazole monomers have been synthesized in a modular manner. Their oxidative polymerization around magnetite nanosized particles has been investigated and optimized toward new magnetic magnetite-polydipyrrole/polydicarbazole nanocomposites (NCs) of a core−shell morphology. These NCs were thoroughly characterized by FT-IR, TGA (Thermal Gravimetric Analysis), low- and high-resolution TEM/HR-TEM microscopies, and Mössbauer spectroscopy along with magnetization studies. Exploiting the versatile COOH chemistry (activation by water-soluble diimides) introduced by the polymeric shell, DNA hybridization experiments have been conducted onto NC surfaces using an efficient blue-colored HRP-based enzymatic screening biological system. Highly parallel NC-supported DNA hybridization experimentations revealed that these NCs presented an interesting potential for DNA-based diagnostic applications.

Introduction

Nanoparticulate materials found extensive applications in various domains such as electronics (data storage), catalysis, and biotechnology/biomedicine.[1−5] Generally, they present a vast range of unique size-related optical, physical, chemical, and magnetic properties that clearly differ from those of similar bulk materials. More specifically for biotechnology/biomedicine applications, hybrid functionalized nanosized materials are constantly developed as essential components of genomics/proteomics-related diagnostic and sensing methodologies.[6] The preparation of novel magnetic nanocomposites (NCs)/nanoparticles of improved properties are another important aspect in biotechnology- and biomedicine-related applications. Magnetically driven separations of small biological components and cells, detoxification of undesirable molecules and antigens, magnetic field-guided delivery of drugs (drug targeting) and genes (gene therapy), relaxation and contrast enhancement in noninvasive magnetic resonance imaging (MRI) of tissues, piezoelectric immunosensors, and magnetic fluid hyperthermia for cancer therapy have been recently disclosed in those areas.[7−14]

Concerning the above stated fields of research, magnetically responsive conducting polymer[15−22] (CP)-based NCs where inorganic magnetic nanosized cores are covered by thin insoluble outer layers of CPs are quite new core−shell materials of underestimated potential.[23,24] Armes and co-workers first oxi-

† Bar-Ilan University.
‡ University of Kent.
§ The Hebrew University.
|| Savyon Diagnostics Ltd.

(1) Arshady, R.; Pouliquen, D.; Halbreich, A.; Roger, J.; Pons, J. N.; Bacri, J. C.; Da Silva, M. d. F.; Hafeli, U. *Microspheres, Microcapsules & Liposomes* **2002**, *5*, 283−329.
(2) Hyeon, T. *Chem. Commun.* **2003**, 927−934.
(3) Hilgendorff, M.; Giersig, M. *NATO Science Series, II: Mathematics, Physics and Chemistry* **2003**, *91*, 151−161.
(4) Willard, M. A.; Kurihara, L. K.; Carpenter, E. E.; Calvin, S.; Harris, V. G. *Encyclopedia of Nanoscience and Nanotechnology* **2004**, *1*, 815−848.
(5) Pellegrino, T.; Kudera, S.; Liedl, T.; Javier, A. M.; Manna, L.; Parak, W. J. *Small* **2005**, *1*, 48−63.
(6) Cao, Y. C.; Jin, R.; Nam, J.; Thaxton, C. S.; Mirkin, C. A. *J. Am. Chem. Soc.* **2003**, *125*, 14676−14677.
(7) *Scientific and Clinical Applications of Magnetic Carriers*; Häfeli, U., Schütt, W., Teller, J., Zborowski, M., Eds.; Plenum Press: New York, 1997.
(8) Safarik, I.; Safarikova, M. *Monatsh. Chem.* **2002**, *133*, 737−759.
(9) Hergt, R.; Hiergeist, R.; Hilger, I.; Kaiser, W. *Recent Research Developments in Materials Science* **2002**, *3*, 723−742.
(10) Berry, C. C.; Curtis, A. S. G. *J. Phys. D: Appl. Phys.* **2003**, *36*, R198−R206.
(11) Jain, K. K. *Expert Review of Molecular Diagnostics* **2003**, *3*, 153−161.
(12) Pankhurst, Q. A.; Connolly, J.; Jones, S. K.; Dobson, J. *J. Phys. D: Appl. Phys.* **2003**, *36*, R167−R181.
(13) Mornet, S.; Vasseur, S.; Grasset, F.; Duguet, E. *J. Mater. Chem.* **2004**, *14*, 2161−2175.
(14) Payne, A. G. *Medical Hypotheses* **2004**, *62*, 718−720.
(15) Bidan, G. *Sens. Actuators B* **1992**, *6*, 45−56.
(16) Deronzier, A.; Moutet, J. C. *Curr. Top. Electrochem.***1994**, *3*, 159−200.
(17) Cosnier, S. *Appl. Biochem. Biotechnol.* **2000**, *89*, 127−138.
(18) Malinauskas, A. *Polymer* **2001**, *42*, 3957−3972.
(19) Gangopadhyay, R.; De, A. *Handbook of Organic−Inorganic Hybrid Materials and Nanocomposites* **2003**, *2*, 217−263.
(20) Rubinson, J. F. *ACS Symp. Ser.* **2003**, *832*, 2−15.
(21) Gangopadhyay, R. *Encyclopedia of Nanoscience and Nanotechnology* **2004**, *2*, 105−131.
(22) Wallace, G. G.; Innis, P. C.; Kane-Maguire, L. A. P. *Encyclopedia of Nanoscience and Nanotechnology* **2004**, *4*, 113−130.

10.1021/ja050285l CCC: $30.25

Scheme 1. Synthesis of DPyr-/DCbz-Based Mono-/Diacid Monomers from L-Lysine Including a Key Aminated Monocarbazole Intermediate

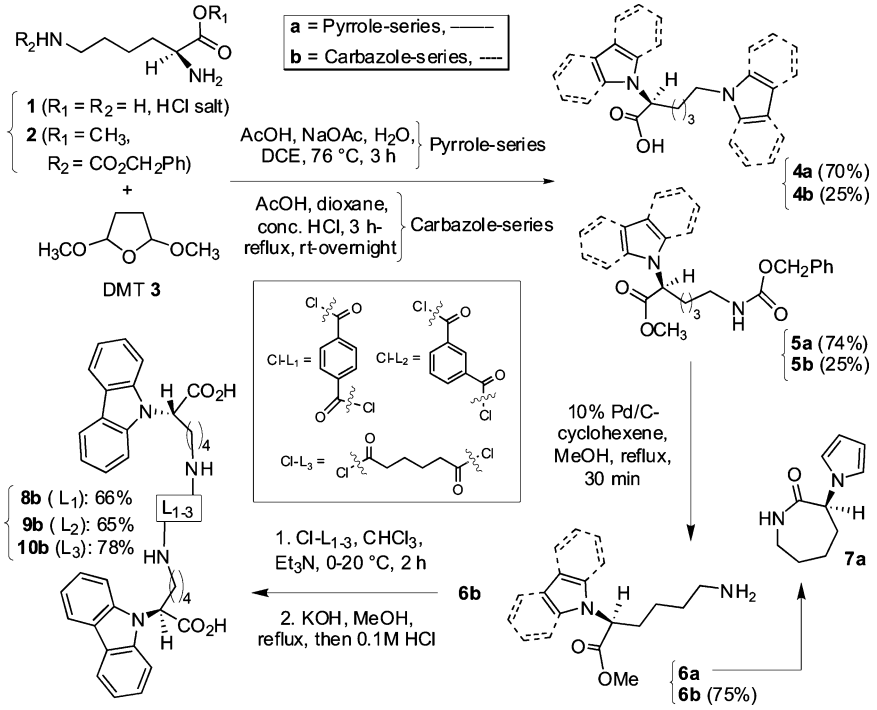

datively deposited *nonfunctional* doped polypyrrole around nanosized silica-magnetite (Fe_3O_4) particles using both aqueous oxidants H_2O_2/Fe^{3+}/HCl and $(NH_4)_2S_2O_8$.[25,26] Resulting colloidally stable core−shell NCs with diameters in the range 100−520 nm displayed superparamagnetism. Much more recently at near completion of our own studies, Peng's group described the fabrication of nanosized ferromagnetic Fe_3O_4-*cross*-linked polyaniline NCs by oxidatively polymerizing aniline (oxidizable monomer) using ammonium peroxodisulfate oxidant $(NH_4)_2S_2O_8$.[27] Related NCs were polydispersed (20−30 nm averaged diameter) and of a core−shell morphology. Even nonmagnetic organic (polystyrene-latex),[28−31] inorganic (SiO_2,[32−38] SnO_2[39]) and metallic (Au)[40,41] cores have been successfully engaged as micro-/nanosized supports to oxidatively polymerize nonfunctional/functional CP precursors in their presence.

Obviously, the full potential of magnetic magnetite-CPs NCs has not yet been fully exploited especially considering heterocyclic *functional* CP precursors built on oxidizable heterocycles different from usual nonfunctional pyrrole or aniline. Accordingly, we wanted to develop such magnetically responsive NCs enabling the *post*polymerization covalent attachment of biological species and more specifically of DNA sequences. For that purpose, we designed and synthesized several new bis-heterocyclic mono- and dicarboxylated dipyrrole (DPyr, indexed **a**) and dicarbazole (DCbz, indexed **b**) monomers to be oxidatively polymerized around magnetite nanoparticles (Schemes 1 and 2). Both DPyr- and DCbz-monomers **4a**−**b** were directly accessible in one step from L-lysine **1** (hydrochloride form) using a modified Clauson−Kaas[42−44] reaction. Other DPyr-/DCbz monomers **15**−**18a**, **8**−**10b**, and **15**−**18b** have been built modularly in order to introduce molecular diversity[45−47] at the monomer level while minimizing the number of synthetic steps to a maximum of 3 or 4 steps. Key structural features included oxidizable monocarboxylated or monoaminated Pyr- and Cbz-containing building blocks arising from L- or D-amino acids and appropriate linkers of variable lengths. C_2-symmetrization operations made use of generally high-yielding stable amide connections between these Pyr- and Cbz-based building blocks and both hydrophilic or hydrophobic diaminated/dicarboxylated linkers $Cl-L_{1-3}/H_2N-L_{4-5}$. Nonproblematic chemical polymerizations of DPyr-monomers around magnetite nanoparticles were expected based on literature results[15−22] and on our own

(23) Armes, S. P. *Curr. Opin. Colloid Interface Sci.* **1996**, *1*, 214−220.
(24) Gangopadhyay, R.; De, A. *Chem. Mater.* **2000**, *12*, 608−622.
(25) Butterworth: M. D.; Armes, S. P. *Polym. Mater.: Sci. Eng.* **1995**, *72*, 300−301.
(26) Butterworth, M. D.; Bell, S. A.; Armes, S. P.; Simpson, A. W. *J. Colloid Interface Sci.* **1996**, *183*, 91−99.
(27) Deng, J.; Ding, X.; Zhang, W.; Peng, Y.; Wang, J.; Long, X.; Li, P.; Chan, A. S. C. *Polymer* **2002**, *43*, 2179−2184.
(28) Lascelles, S. F.; Armes, S. P. *J. Mater. Chem.* **1997**, *7*, 1339−1347.
(29) Barthet, C.; Armes, S. P.; Lascelles, S. F.; Luk, S. Y.; Stanley, H. M. E. *Langmuir* **1998**, *14*, 2032−2041.
(30) Cairns, D. B.; Armes, S. P.; Bremer, L. G. B. *Langmuir* **1999**, *15*, 8052−8058.
(31) Khan, M. A.; Armes, S. P. *Langmuir* **1999**, *15*, 3469−3475.
(32) Maeda, S.; Armes, S. P. *J. Colloid Interface Sci.* **1993**, *159*, 257−259.
(33) Maeda, S.; Armes, S. P. *J. Mater. Chem.* **1994**, *4*, 935−942.
(34) Maeda, S.; Corradi, R.; Armes, S. P. *Macromolecules* **1995**, *28*, 8, 2905−2911.
(35) Pope, M. R.; Armes, S. P.; Tarcha, P. J. *Bioconjugate Chem.* **1996**, *7*, 436−444.
(36) McCarthy, G. P.; Armes, S. P.; Greaves, S. J.; Watts, J. F. *Langmuir* **1997**, *13*, 3686−3692.
(37) Han, M. G.; Armes, S. P. *Langmuir* **2003**, *19*, 4523−4526.
(38) Azioune, A.; Ben Slimane, A.; Hamou, L. A.; Pleuvy, A.; Chehimi, M. M.; Perruchot, C.; Armes, S. P. *Langmuir* **2004**, *20*, 3350−3356.
(39) Maeda, S.; Armes, S. P. *Synth. Met.* **1995**, *69*, 499−500.
(40) Marinakos, S. M.; Novak, J. P.; Brousseau, L. C., III; House, A. B.; Edeki, E. M.; Feldhaus, J. C.; Feldheim, D. L. *J. Am. Chem. Soc.* **1999**, *121*, 8518−8522.
(41) Marinakos, S. M.; Shultz, D. A.; Feldheim, D. L. *Adv. Mater. (Weinheim, Germany)* **1999**, *11*, 34−37.
(42) Périé, K.; Marks, R. S.; Szumerits, S.; Cosnier, S.; Lellouche, J.-P *Tetrahedron Lett.* **2000**, *41*, 3725−3729.
(43) Elming, N.; Clauson-Kaas, N. *Acta Chim. Scand.* **1952**, 867−874.
(44) Périé, K.; Strokhin, V.; Marks, R. S.; Lellouche, J.-P. *Novel Approaches in Biosensors and Rapid*, Diagnostic Assays. 43rd OHOLO Conference, Eilat, Oct. 10−14, 1999; Liron, Z., Bomberg, A., Fisher, M., Eds; Kluwer Academic/Plenum Publishers: New York, 2001; pp 225−233.
(45) Meyers, H. V. *Biology-Chemistry Interface* **1999**, 271−287.
(46) Weber, L. *Methods and Principles in Medicinal Chemistry*; Clark, D. E., Ed.; Wiley-VCH: 2000; Vol. 8, pp 137−157.
(47) Wright, D. L.; Orugunty, R. S.; Robotham, C. V. *Organic Synthesis: Theory and Applications* **2001**, *5*, 197−254.

Scheme 2. DPyr-/DCbz-Containing Diacid Monomers from L-Aspartic and Glutamic Amino Acids

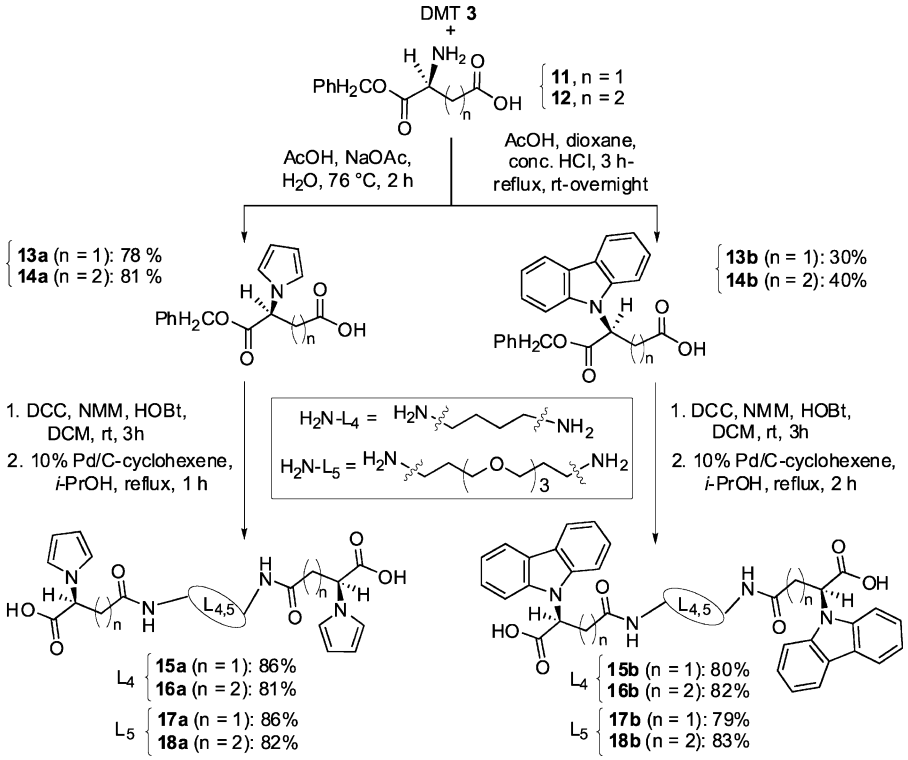

experience. On the contrary and most importantly, the bis-heterocylic chemical design of DCbz-monomers that are more difficult to oxidize is worth mentioning. Indeed, the electrochemical polymerization of *N*-susbtituted monocarbazole monomers is known to produce only short useless tetrameric oligomers soluble in electrochemical media.[48,49] However, overcoming this limitation, we recently successfully electrosynthesized stable amine-sensitive polydicarbazole (polyDCbz) films onto Au microelectrodes.[42] Such polyDCbz-films were produced from bis-heterocyclic *N*-pentafluorophenyl and *N*-hydroxysuccinimidyl/phthalimidyl esters of DCbz-monomer **4b** (Scheme 1) enabling the *post*-electropolymerization covalent attachment of polyphenol and glucose oxidases.[50−52] Most likely, the specific bis-heterocyclic chemical design of monomer **4b** (ester forms) allowed reticulation of the corresponding polyDCbz-polymer that resulted in an improved stability of films. Moreover and in addition to monomer **4b** (acid form), two other similarly designed DCbz-monomers (acid form) **8**−**9b** have been successfully oxidized chemically around magnetite nanoparticles. It afforded carboxylated magnetite-polyDCbz NCs of a core−shell sheetlike morphology (20−40 nm averaged size).[53]

Altogether, these two convergent results prompted us to investigate more deeply the preparation, characterization, and use in sensitive DNA hybridizations of novel magnetic magnetite-polyDPyr/polyDCbz NCs arising from a much wider range of carboxylated bis-heterocyclic DPyr-/DCbz-monomers. Their modular chemical design authorized a high structural diversity for monomers that emphasized the respective roles of both different heterocycles (Pyr and Cbz) and hydrophilic/hydrophobic linkers on the performances of corresponding NCs. Upon DNA hybridization, sensitivity features of a model DNA analyte as well as the nonspecific binding issues were also examined. The obtained results pointed out the great importance of the concept of molecular diversity for engineering functional polyDPyr-/polyDCbz- shell outer layers of magnetic NCs.

Experimental Section

Amino acid precursors were purchased from Bachem. DMT (2,5-dimethoxytetrahydrofuran) **3**, HOBt (1-hydroxybenzotriazole), DCC (dicyclohexylcarbodiimide), and *N*-methylmorpholine (NMM) were used as supplied from Acros. High-field ^{1}H and ^{13}C Fourier Transform NMR spectra were obtained from a Bruker DMX 300 machine (300 and 75 MHz respectively). IR spectral data were collected using a Bomen-Hartman & Braun Instrument using KBr pellets (transmission better than 85%, see the Supporting Information (SI) for details on sample preparation). Formvar carbon 400 mesh Cu (SPI Supplies West Chester, USA) and carbon-free 400 mesh Au grids (Agar Scientific Ltd., U. K.), respectively, have been used for low- and high-resolution TEM microphotographs. Microphotographs were obtained from both JEOL-1200EX and JEOL-JEM2010 instruments (Oxford Instruments, accelerating voltage 200 kV, Gatan CCD camera). TGA graphs were run on a TGA-Mettler apparatus (TG-50 DSS50 model) with temperature profile settings being 25−130 °C at 20 °C/min, at 130 °C for 15 min and then onward to 800 °C at 15 °C/min under N_2. C,H,N-Elemental analyses were performed on an EA 1110/CHNS-O CE instrument, and data were corrected for oxygen. Saturation magnetizations M_s and coercivity factors H_c were measured from an Oxford VSM system Magnetometer equipped with an Aerosonic VSM 3001 controller. Mössbauer spectra were obtained at both 90 and 300 K temperatures using a conventional Mössbauer spectrometer and a 30 mCi ^{57}Co (Rh) radioactive source. Spectra were computer-fitted with Lorentzian lines,

(48) Helary, G.; Chevrot, C.; Sauvet, G.; Slove, A. *Polym. Bull.* **1991**, *26*, 131−138.
(49) Desbene-Monvernay, A.; Lacaze, P. C.; Delamar, M. *J. Electroanal. Chem.* **1992**, *354*, 241−246.
(50) Cosnier, S.; Marks, R. S.; Lellouche, J.-P.; Périé, K.; Fologea, D.; Szunerits, S. *Electroanalysis* **2000**, *12*, 1107−1112.
(51) Cosnier, S.; Szunerits, S.; Marks, R. S.; Lellouche, J.-P.; Périé, K. *J. Biochem. Biophys. Methods* **2001**, *50*, 65−77.
(52) Cosnier, S.; Le Pellec, A.; Marks, R. S.; Périé, K.; Lellouche, J.-P. *Electrochem. Commun.* **2003**, *5*, 973−977.
(53) Lellouche, J.-P.; Perlman, N.; Joseph A.; Govindaraji S.; Buzhansky, L.; Yakir, A.; Bruce, I. *Chem.* Commun. **2004**, 560−561.

with line widths, quadrupole splittings, isomer shifts, and magnetic hyperfine fields being free parameters. Magnetite particles were dispersed during NC fabrication using a Bransonic ultrasonic cleaner (2510E MTH model, 42 kHz at full power).

Specific Reagents, Buffers, and Washing/Assay Solutions for DNA Hybridizations. PBS buffer (*p*H 7.0): prepared from Dulbecco's Phosphate Buffered Saline (Sigma). 0.4 M MES (*p*H 5.0): prepared using 2-morpholinoethanesulfonic acid hydrate 99%, adjusted to pH 5.0 by addition of 10 M NaOH and stored at 4 °C. TNET buffer (*p*H 7.5): prepared from a mixture of 10 mM Tris-HCl, 0.5 M NaCl, 1 mM EDTA, and 0.02% Tween-20. Washing solution: prepared from a mixture of 3 M NaCl and 2 M Tris-HCl (pH 7.5). Assay solution: prepared from a mixture of 154 mM NaCl, 50 mM Tris-HCl (pH 7.8), 0.5% BSA, and 0.1% Tween 20. EDC: *N*′-(3-(dimethylamino)propyl)-*N*-ethylcarbodiimide hydrochloride, >98% purity (Aldrich).

Results and Discussion

Synthesis of Carboxylated DPyr-/DCbz-Monomers. Monocarboxylate DPyr- and DCbz-based monomers **4a**−**b** were synthesized in one step starting from L-lysine (hydrochloride salt) **1** and 2,5-dimethoxytetrahydrofuran **3** (DMT) according to a modified Clauson−Kaas reaction[42−44] (Scheme 1). Basically, two different sets of sligthly acidic conditions were separately optimized (**4a**: AcOH, NaOAc/H_2O, 1,2-CH_2ClCH_2-Cl (DCE), 76 °C, 3 h, 70% yield; **4b**: AcOH, concentrated HCl, dioxane, reflux, 3 h then overnight at room temperature, 25% yield). Accordingly and in four steps from starting ϵ-NH(*Z*)-protected L-lysine **2** (*Z*: benzyloxycarbonyl group), two aromatics and one alkyl (butyl) C_2-symmetrical dicarboxylate DCbz-monomers **8**−**10b** were readily synthesized through the pivotal monocarbazole monoamine intermediate **6b** (Scheme 1, **8**−**9b**: 12% global yield for each monomer, **10b**: 15% global yield) using key C_2-symmetrization amidations ($CHCl_3$, Et_3N, Cl-L_{1-3} linkers, 0−20 °C, 2 h, 68−72% yields). Aromatic and alkyl linkers arose from tere- (*para* substitution), isophthaloyl (*meta* substitution), and adipoyl (hexyl linker) dichlorides. Similar attempts to prepare the pyrrole ϵ-NH_2 analogue **6a** of the carbazole intermediate **6b** from the ϵ-NH(*Z*)-protected pyrrole compound **5a** were unsuccessful due to its intrinsic instability after *Z*-group deprotection by transfer hydrogenolysis (Scheme 1, 10% Pd/C, cyclohexene, MeOH, reflux, 30 min). Indeed, the resulting deprotected ϵ-aminated intermediate **6a** could not be obtained pure since it readily and consistently cyclized intramolecularly toward the corresponding seven-membered pyrrole lactam **7a** during manipulation (**6a:7a** = 4:1 assayed by high-field ^{1}H NMR for a quasi-quantitative 91% recovery yield after separation from reaction mixture). This intramolecular amidation did not occur for the sterically more hindered Cbz-based intermediate **6b**, therefore, allowing corresponding C_2-symmetrization amidations as described above (Scheme 1).

To exclude these limiting intramolecular amidations, two novel amino acid starting blocks, e.g., benzyl esters of L-aspartic and glutamic acids, have been similarly reacted with DMT **3** according to the same modified Clauson−Kaas reaction (Scheme 2).

Uneventfully, both former sets of acidic conditions afforded Pyr- and Cbz-containing monomers **13**−**14a** and **13**−**14b** (mono benzyl esters) building on aspartic and glutamic acid skeletons (Scheme 2; **13**−**14a** (n = 1, 2): AcOH, NaOAc/H_2O, 76 °C, 2 h, 78 and 81%; **13**−**14b** (n = 1, 2): AcOH, dioxane at reflux, 3 h then overnight at 20 °C, 30 and 40%). C_2-symmetrization couplings of these benzylated acids could proceed readily with both diamine linkers H_2N-L_{4-5}, e.g., lipophilic 1,4-diaminobutane and hydrophilic 4,7,10-trioxa-1,13-tridecanediamine using a DCC−HOBt amide coupling system (H_2N-L_{4-5}, DCC, HOBt, *N*-methyl morpholine (NMM), CH_2Cl_2, room temperature, 3 h). Final deprotection of resulting symmetrized benzyl esters by transfer hydrogenolysis (10% Pd/C, cyclohexene, *i*-PrOH, reflux, 1 or 2 h) completed the corresponding synthetic sequences. It afforded the targeted dicarboxylate DPyr-/DCbz-monomers **15**−**18a/b** (acid forms) in three steps from starting benzylated amino acids **11**−**12**. Consistent with previous observations, medium to good overall yields in DPyr-/DCbz-monomers depended on heterocyclic DPyr- or DCbz-series (DPyr-**15**−**18a**: 66−70% overall yields, DCbz-**15**−**18b**: 24−34% overall yields).

All these DPyr-/DCbz-monomers have been fully characterized, their chemical structures confirmed, and purities checked before the fabrication of corresponding NCs by appropriate analytical means (thin-layer and high-performance liquid chromatographies, optical rotations[54]) and spectroscopic analyses (FT-IR, 1D/2D-high-field ^{1}H/^{13}C NMR, low- and high-resolution FAB-MS, S-2 in the SI section). Interestingly and for all DPyr-/DCbz-monomers, connecting chains separating heterocyclic units presented different lengths and lipophilicity/hydrophilicity characteristics that could have a major importance regarding fabrication and properties of polymeric outer layers deposited onto magnetite nanoparticles.

Preparation of Magnetite-Carboxylated PolyDPyr-/PolyDCbz-Nanocomposites. Concerning preparation of magnetite-polyDPyr/-polyDCbz NCs, nanosized magnetite particles onto which monomeric CP-precursors were polymerized have been prepared by a modified Sugimoto method.[55,56] The oxidative hydrolysis of iron(II) sulfate heptahydrate $FeSO_4 \cdot 7H_2O$ by KNO_3 in an alkaline KOH medium under nitrogen gave free-flowing brilliant black magnetite sheetlike nanoparticles of mean size 20−40 nm (low-resolution TEM analysis). Magnetite nanoparticles were characterized by FT-IR spectroscopy (KBr pellet) that showed strong characteristic peaks at 411 and 584 cm^{-1}. Additionally, a broad and strong peak at 3422 cm^{-1} indicated the presence of surface Fe−OH hydroxyl groups.[55,56] Variations of the intensity of this specific IR absorption peak allowed a simple followup of surface modifications occurring onto magnetite nanoparticles during NC fabrication. ^{57}Fe Mössbauer spectroscopy also confirmed the absence of maghemite (γ-Fe_2O_3) as an oxidation end-product of magnetite. Magnetite nanoparticles could be dispersed and stored for some days in neutral water at 4 °C at a concentration of 46.7 g/L as a stock solution. Aliquots from this stock solution were further diluted before use in each set of polymerization experiments (see typical procedures, S-1 in the SI).

Salient Features of the Methodology of NC Preparation. Results obtained during this work clearly emphasized *three* salient features of NC preparation, confirming previous data obtained for a much shorter range of monomers.[53] First, oxidative polymerizations of DPyr- and DCbz-monomers in the presence of magnetite nanoparticles needed minimal monomer and oxidant solubilities in aqueous or nonaqueous media. For

(54) All chemical intermediates and monomers are optically pure (HPLC separation of diastereomers according to ref 42). It should also be noticed that, after C_2-symmetrization amidations, meso diasteromers were never detected (^{13}C/^{1}H NMR) implying excellent enantiomeric purities (ee ~97%).
(55) Sugimoto, T.; Matijevic, E. *J. Colloid Interface Sci.* **1980**, *74*, 227−243.
(56) Taylor, J. I.; Hurst, C. D.; Davies, M. J.; Sachsinger, N.; Bruce, I. J. *J. Chromatogr., A* **2000**, *890*, 159−166.

example, DCbz-monomers **15b** and **17b** could not be polymerized, since they were totally insoluble in any organic or water-miscible organic solvent. Preliminary screening studies were conducted with the monocarboxylated monomers **4a**−**b**. Polymer deposits in resulting NCs were followed by TGA (Thermal Gravimetric Analysis, 200−750 °C temperature range) and FT-IR analyses. Several polymerization parameters were examined and included different (i) polymerization times (1−6 h range), (ii) mono- or bis-electronic oxidants, (iii) molar/weight ratios of DPyr- and DCbz-monomers/magnetite nanoparticles, (iv) polymerization solvents (alcohols, acetone, acetonitrile, dimethylformamide, and respective aqueous mixtures), (v) medium temperatures (in the range of 25−55 °C) whether using ultrasounds or not (ultrasonic cleaner Bransonic at full 42 Khz power, 2510E MTH model), and finally (vi) magnetite concentrations (0.5−5% w/v range at constant experiment volume). Therefore, *two* different polymerization media have been specifically disclosed for optimal polymerization of DPyr- and DCbz-monomers (45/55 v/v H_2O/CH_3OH mixture and pure acetone, respectively; see corresponding procedures in the SI) after process extension to the full set of monomers.

The absolute requirement for ultrasonic irradiation of polymerization media was a second salient feature. It allowed improved DPyr-/DCbz-monomer and oxidant dispersion/solubilization at an optimal constant medium temperature of 55 °C. Moreover, produced nanosized NCs[1−4] showed minimal aggregation for all tested DPyr-/DCbz-monomers (low-resolution TEM analysis).

A third feature was related to selected mono- and bis-electronic oxidants optimal for both series of DPyr-/DCbz-monomers. On one hand, all tested DPyr-monomers **4a** and **15**−**18a** were best polymerized by $FeCl_3$ and ammonium peroxodisulfate $(NH_4)_2S_2O_8$ with the last oxidant being preferred (cleaner magnetite-polyDPyr NCs). On the other hand, DCbz-monomers **4b**, **8**−**10b**, **16b**, and **18b** could be efficiently polymerized only when using the Ce(IV) salt CAN ($(NH_4)_2Ce(NO_3)_6$[53] (see typical procedures for NC preparation, S-1 in the SI). Beyond the use of oxidants specific to each monomer series, main protocol differences related to (i) optimal polymerization media, e.g., a 45/55 v/v H_2O/CH_3OH mixture for DPyr-based monomers **4a** and **15**−**18a** and pure CH_3COCH_3 for the more hydrophobic DCbz-based ones **4b**, **8**−**10b**, **16b**, and **18b**, and (ii) optimal ultrasound-assisted polymerization times, e.g., *1 h* for DPyr-based monomers versus *5 h* for DCbz-based ones.

Nanocomposite Characterization. Magnetically responsive magnetite-polyDPyr and -polyDCbz NCs have been thoroughly characterized using a range of analytical and spectroscopic methods that included FT-IR and ^{57}Fe Mössbauer spectroscopies, C,H,N-elemental and TGA thermogravimetric analyses, magnetism measurements, and finally low- and high-resolution TEM microscopies with energy-dispersive X-ray elemental microanalysis (EDAX). Additionally as discussed later on, a highly efficient DNA-based biological parallel screening system helped to characterize and evaluate prepared magnetic NCs via specific binding/nonspecific properties of structurally versatile polymeric coverages. Covalent attachment of a model aminated 20-*mer* DNA capture probe onto magnetic NCs made use of the versatile COOH chemistry through carboxylate activation by the water-soluble carbodiimide EDC.[57−59] Thereafter, DNA hybridizations occurring onto NC surfaces were specifically examined using an amplifying blue-colored HRP-based enzymatic system (HRP: horseradish peroxidase) allowing detection and quantification of optically read signal outputs.

FT-IR Studies: FT-IR spectra of all the *eleven* prepared NCs were analyzed and compared with those of magnetite and corresponding monomers (see S-3 in the SI). FT-IR spectra of all magnetite-polyDPyr/polyDCbz NCs were found to be very similar. They included mixed absorption peaks characteristic of both freshly prepared magnetite (ν: 1083−1099, 1017−1024, 568−585 cm^{-1}) and of polyDPyr- and polyDCbz-polymeric systems {ν: 2850−2922 and 2958−2964 (δ_{Csp3-H}), 1650−1750 ($\nu_{C=O}$, carboxyl), 1454−1558 ($\nu_{Csp2-Csp2}$, polypyrrole and polycarbazole aromatics), 1258−1264 ($\nu_{(C=O)-O}$, acid), 800−808 (δ_{Csp2-H}, out of plane stretching) cm^{-1}}. As cited before, the intensity of the large absorption peak corresponding to surface Fe−OH hydroxyl groups of magnetite ($\nu = 3422$ cm^{-1}) in prepared NCs was greatly reduced. It clearly suggested that carboxylated polyDPyr-/polyDCbz-outer layers should strongly interact with magnetite Fe−OH hydroxyl groups through respective interactions of type Fe−OH/COOH polymer groups (metallic ester bond). Current available literature[60] in the field supported this result disclosing similar examples of strong interactions between carboxylated organic ligands and metal oxides. On the other hand, more importantly, strong carbonyl stretching vibrations appearing at $\nu_{C=O} = 1630-1750$ cm^{-1} were rather indicative of free carboxylates useful for the covalent immobilization of any amine modified capture bioprobes.

TEM Analysis. Low-resolution TEM microphotographs have been obtained for all the prepared NCs. Notably, they indicated that our fabrication process involving ultrasonication altered neither the sheetlike polygonal morphology nor the average size (20−40 nm) that characterized starting magnetite nanoparticles. Furthermore, smoother nonsharp-edged morphological features of NCs versus starting magnetite nanoparticles pointed out the likely presence of polymeric polyDPyr-/polyDCbz-adlayers around magnetite nanoparticles. Mixed structures of the type discrete polyDPyr and polyDCbz particulate-magnetite nanoparticles could not be also detected. These observations combined with FT-IR analyses of NCs emphasized the likely core−shell morphology of magnetite-polyDPyr/-polyDCbz NCs. An absolute proof for that core−shell morphology *for all prepared NCs* arose from HR-TEM analyses performed together with elemental energy-dispersive X-ray measurements (EDAX analyses). Illustrative HR-TEM images (Figure 1and S-4 in the SI) of four selected NCs magnetite-polyDPyr(**4a**), -polyDCbz-(**4b**), -polyDPyr(**16a**), and -polyDCbz(**16b**) clearly showed magnetite crystals covered by more or less uniform amorphous polyDPyr-/DCbz-adlayers.

For these NCs, adlayer thicknesses varied in a 5−7.5 nm range. EDAX elemental analyses performed onto NC samples deposited onto 400 mesh *carbon-free* gold grids consistently showed iron-poor carbon-enriched crystal edges versus iron-rich carbon-poor crystal centers after element calibration (INCA software). In fact, these observations were consistent with the relatively low quantity of polyDPyr and polyDCbz polymers deposited onto magnetite nanoparticles independently of DPyr-/DCbz-type of monomers (∼18−32% w) as discussed later on (TGA and C,H,N-elemental analyses of nanocomposites).

(57) Staros, J. V. *Biochemistry* **1982**, *21*, 3950−3955.
(58) Gibson, F. S.; Park, M. S.; Rapoport, H. *J. Org. Chem.* **1994**, *59*, 7503−7507.
(59) Grayson, I. *Speciality Chemicals* **2000**, *20*, 86−88.
(60) Kataby, G.; Cojocaru, M.; Prozorov. R.; Gedanken A. *Langmuir* **1999**, *15*, 1703−1708 and references therein.

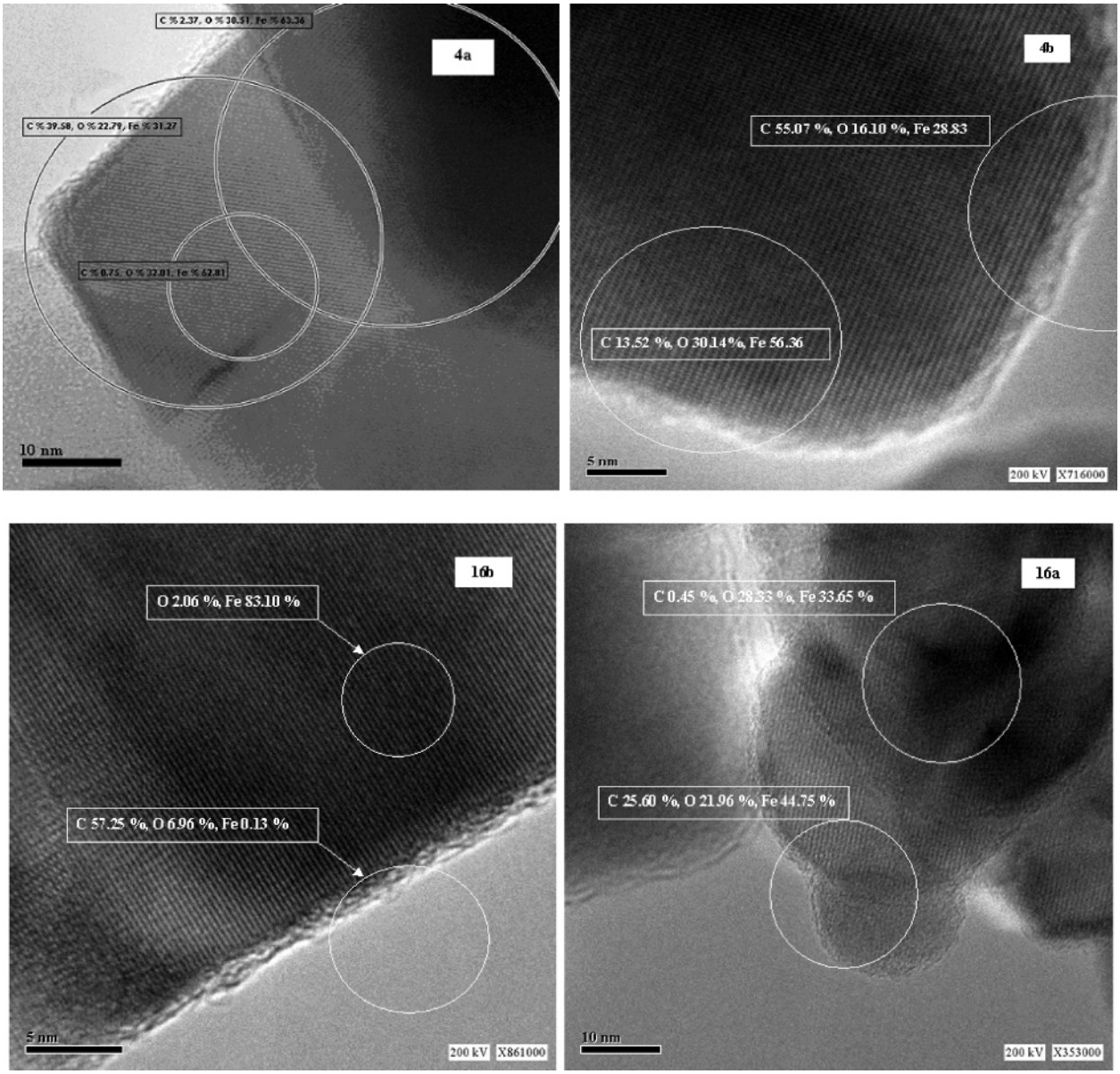

Figure 1. HR-TEM microphotographs of selected magnetite-polyDPyr/-polyDCbz nanocomposites.

TGA and C,H,N-Elemental Analyses. TGA analyses of all NCs were carried out in the temperature range 200−750 °C with the specific temperature profile indicated in the Experimental Section (Experimental Section, TGA curves and Table S-6 in the SI). Both types of magnetite-polyDPyr and -polyDCbz NCs showed different patterns of two-step profiles of weight losses (TGA curves, S-6 in the SI). Weight losses between 250 and 400 °C (first step) could be due to evaporation/decomposition of shorter oligomeric polymer chains, while end polymer decomposition/burning occurred in a second step between 400 and 700 °C depending on NCs. Both polyDPyr- and polyDCbz-based NCs lead to polymer deposits in a w/w range of 18−30% and 21−31%, respectively.

C,H,N-Elemental analysis data corrected for oxygen (Table S-6 in the SI) were found quite consistent with these NC compositional data and, therefore, allowed to check for data homogeneity. More specifically and except the atypical TGA curve of the magnetite-polyDCbz(**16b**) NC, other magnetite-polyDCbz NCs displayed one tightly grouped set of very similar TGA curves that appeared independent of monomer structures.

Regarding polyDPyr-based NCs, the magnetite-polyDPyr-(**16a**) NC also displayed an atypical TGA curve when compared to other polyDPyr-based NCs. Contrary to the former polyDCbz-series of NCs, TGA graphs of polyDPyr-based NCs were found quite distinct most likely pointing out a greater influence of DPyr-monomer structures on the stability of corresponding polyDPyr-adlayers to heat.

Magnetization Studies. Bulk magnetization against applied magnetic field experiments have been measured at 300 K for all fabricated lyophilized magnetic NCs. Magnetization profiles (Figure 2and Table S-7 in the SI) were very similar and showed hystereses with coercivity factors H_c in a low to medium range of 35−132 Oe. For that reason, these NCs cannot be strictly considered as superparamagnetic nanocomposites. Saturation magnetizations M_s have been observed in a range of 32−55 emu/g that were lower than the known reported value of 92−98 emu/g of pure magnetite. Most likely, it resulted from the compositional modification of core magnetite due to oxidative polymerization processes. In fact, inorganic magnetic cores were

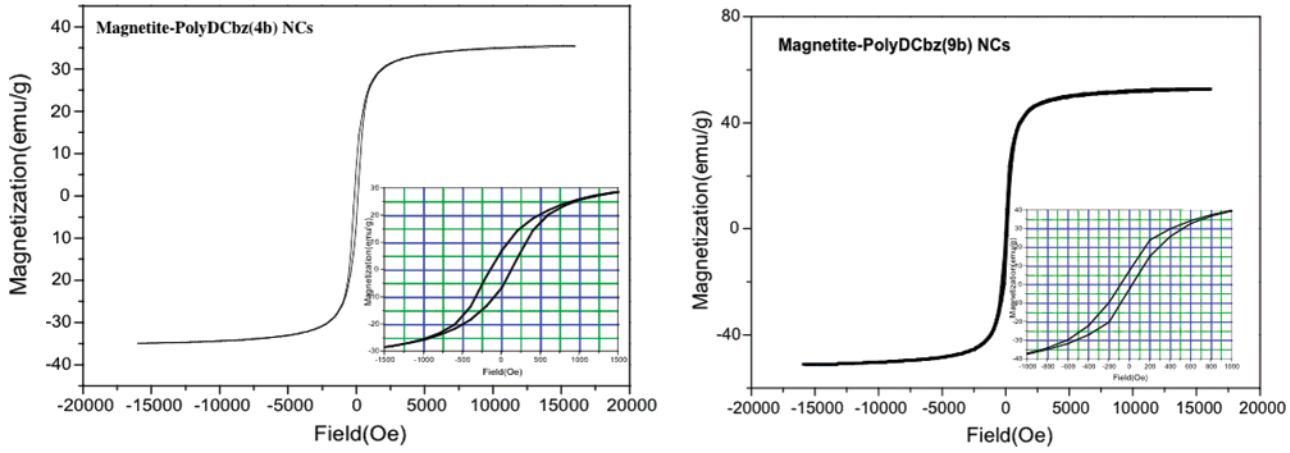

Figure 2. Selected magnetization profiles of magnetite-polyDCbz(**4b**) (M_s: 35 emu/g, coercivity H_c: 132 Oe) and magnetite-polyDCbz (**9b**) (M_s: 52 emu/g, coercivity H_c: 35 Oe) nanocomposites.

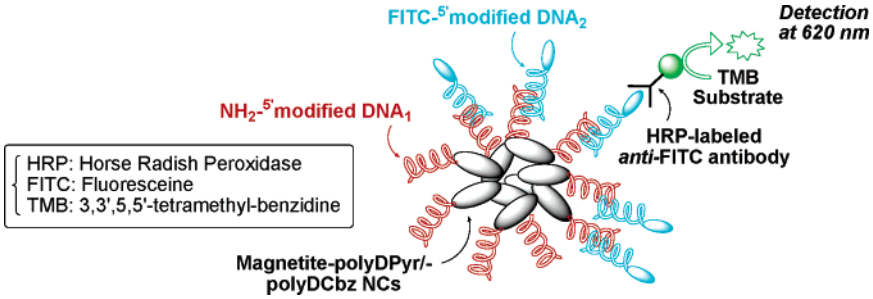

Figure 3. Biological DNA-based screening system involving carboxylated magnetite-polyDPyr/polyDCbz nanocomposites.

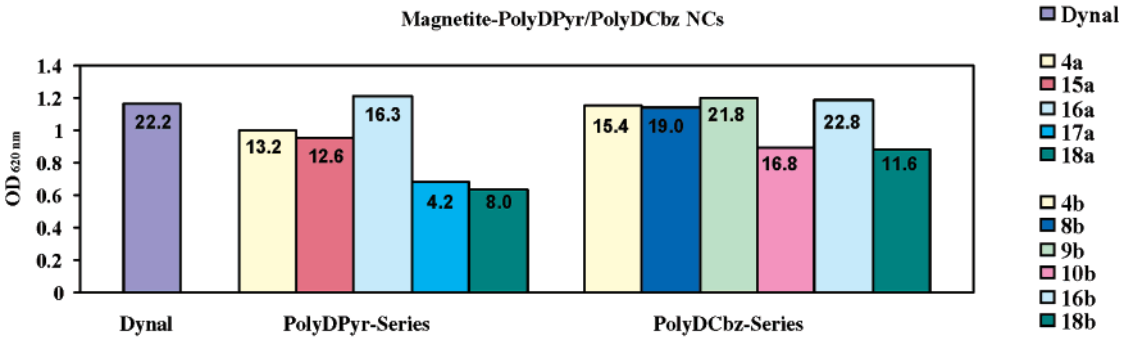

Figure 4. Comparative charts of the efficiency (SB/NSB ratio) of FITC-5′labeled DNA_2 capture at a concentration of 10^{-7} M by magnetite-polyDPyr/polyDCbz nanocomposites.

formed of less magnetic nonstoichiometric magnetite $Fe_{3-x}O_4$ ($0 \leq x \leq 0.33$) as determined by ^{57}Fe Mössbauer analysis at 300 K (obtention of two superposed magnetic subspectra compatible with Fe^{3+} and $Fe^{2.5+}$ atoms located in tetrahedral and octahedral sites, respectively, in different relative intensities, Figure S-5 in the SI). Interestingly, less magnetic NCs of higher coercivity factors were consistently found in the polyDCbz-series due to longer polymerization times, e.g., 5 h versus 1 h for the polyDPyr-series of nanocomposites meaning a more pronounced oxidation of the starting magnetite core.

Covalent Attachment of an NH_2-5′Modified DNA_1 Sequence and Hybridization Studies. Once characterized satisfactorily by the range of methods cited previously, polyDPyr-/polyDCbz-NCs have been screened in a parallel mode using a simple powerful DNA-based biological system (Figure 3 and S-1 in the SI). This DNA-based screening system comprised the covalent attachment of an amine modified single-strand DNA sequence onto NC surfaces and its hybridization to a second complementary DNA sequence. NC-supported DNA hybridizations were characterized and quantified by reading optical outputs generated by an enzymatic amplifying system. For that purpose, an amine modified 20-*mer* DNA probe DNA_1 ($H_2N-(CH_2)_{12}$-5′GCACTGGGAGCATTGAGGCT) that characterized the 20210 mutation in the Human Factor II gene (G → A single oligonucleotide mutation at position 20210)[61,62] has been chosen as a capture DNA probe.

Accordingly, carboxylated magnetite-polyDPyr/polyDCbz NCs were treated with the water-soluble carbodiimide EDC (*N*′-(3-(dimethylamino)propyl)-*N*-ethylcarbodiimide hydrochloride)[59] in a 0.4 M MES buffer medium (pH 5.0, 2 h incubation at 20 °C) to activate surface COOH groups. Then, activated NCs were reacted with the NH_2-5′modified DNA_1 probe toward

(61) Poort, S. R.; Rosendaal, F. R.; Reitsma, P. H.; Bertina, R. M. *Blood* **1996**, *88*, 3698−3703.
(62) Vicente, V.; Gonzalez-Conejero, R.; Rivera, J.; Corral, J. *Haematologica* **1999**, *84*, 356−362.

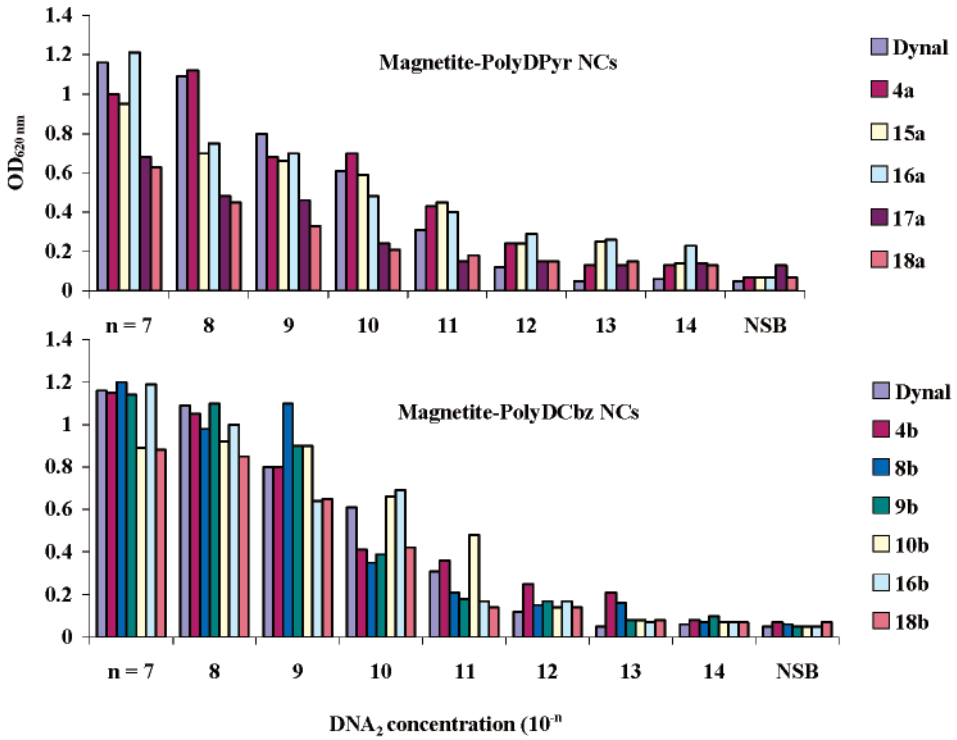

Figure 5. Comparative charts for magnetite-polyDPyr/polyDCbz nanocomposites at decreasing concentrations of the FITC-5′labeled DNA_2 model analyte.

DNA_1-decorated magnetic polyDPyr-/polyDCbz-NCs via covalent amide bonding.[63]

The successful covalent modification of NCs by the probe DNA_1 was confirmed by further hybridizations with a fluoresceine-labeled *anti*-sense 20-*mer* complementary DNA_2 strand (fluoresceine (FITC)-triethyleneglycol linker-5′AGCCTCAATGCTCCCAGTGC, 1 h, 60 °C). After hybridization (TNET buffer, pH 7.5), the NCs were incubated with an *anti*-FITC HRP-labeled mouse monoclonal antibody (HRP: horseradish peroxidase, 20 min, 20 °C) to enable an enzyme-based colored detection of NC-supported DNA hybridizations. Accordingly, this NC-immobilized amplifying enzymatic construct was added and reacted with the HRP colorless substrate TMB (3,3′,5,5′-tetramethylbenzidine). TMB enzymatic oxidation (1.5 min, 20 °C) afforded blue-colored visible optical outputs that were read in parallel (96-well plastic microtiter plate) at 620 nm using an ELISA reader. Resulting measured optical densities (ODs) related to the total amount of FITC-DNA_2 analyte being recognized by DNA_1-decorated NCs (Total Binding: TB) through hybridization-based specific (specific binding: SB) and nonspecific interactions (nonspecific binding: NSB). Parallel experiments were also conducted by omitting the FITC-DNA_2 incubation step with the same DNA_1-decorated NCs. It allowed us to estimate the affinity of DNA_1-decorated magnetite-polyDPy/-polyDCbz NCs to physically adsorb (nonspecific binding: NSB) the reporter *anti*-FITC HRP-labeled mouse antibody. For each tested NC, specific and nonspecific OD values were averaged outputs of six parallel experiments in order to minimize data dispersion. Indeed, OD variations were always observed to be less than 5−8%. Specific binding (SB = TB − NSB)/NSB ratios that were indicative of NC efficiency were calculated and compared with parallel similarly processed commercial micrometric COOH-Dynabeads M-270 (Φ 2.8 μm, Dynal AS, Oslo, Norway),[64] which have been commonly used for magnetism-driven suspension assays.

In a first series of DNA hybridization experiments, concentrations of both complementary FITC-5′labeled -DNA_2 probe and tested NCs were fixed at 10^{-7}M and at 1.0% w/v (50 μg per ELISA microtiter plate well), respectively (S-1 in the SI). From careful examination of resulting SB/NSB ratios (Figure 4), it was found that *two* magnetite-polyDCbz NCs namely, magnetite-polyDCbz(**9b**), and -polyDCbz(**16b**) NCs were as efficient as COOH-Dynabeads in specifically capturing the model analyte FITC-5′labeled DNA_2. Calculated averaged SB/NSB ratios were in a high 21.8−22.8 range. In contrast, all tested magnetite-polyDPyr NCs were found less efficient than standard COOH-Dynabeads with SB/NSB ratios being in a low to medium 4.2−16.3 range.

In this later series, only the magnetite-polyDPy(**16a**) NC had managed to have a decent 16.3 SB/NSB ratio against 22.2 obtained for standard COOH-Dynabeads. Another interesting feature seemingly resulting from monomer design has also been discerned. Both pairs of magnetite-polyDPyr(**16a**)/polyDCbz-(**16b**) and magnetite-polyDPyr(**18a**)/polyDCbz(**18b**) NCs prepared from DPyr-/DCbz-monomers **16/18a−b** showed remarkably different performances. The first pair building on an hydrophobic 1,4-diaminobutane linker at monomer level was

(63) DNA_1 loading for both types of polyDPyr-/polyDCbz-modified NCs and Dynabeads was similar, e.g., 1.2 nmol of DNA_1/mg of NCs/Dynabeads. This is supported by the fact that both CP-modified nanocomposites and Dynabeads possessed concentrations of accessible COOH groups of 36−54 and 150 mmol, respectively, that much exceeded the quantity of DNA_1 engaged in the loading step. Reversed-phase HPLC checking of corresponding *post*coupling washings did not allow detection of any unbound DNA_1 probe (results to be reported in a separate forthcoming publication involving biology-related data).

(64) Dynabeads M-270 (carboxylic acid form, 2.8 μm diameter, 2−5 m^2/g specific area) are superparamagnetic beads composed of highly cross-linked polystyrene with a magnetic iron oxide material precipitated and trapped in evenly distributed pores. A hydrophilic outer layer of glycidyl ether provides functional carboxylate groups (150 μmol/g beads). The iron content of beads is 15% w/w for a magnetic mass susceptibility in a 88−126 × 10^{-6} m^3/g range.

found more efficient (SB/NSB = 16.3 and 22.8) than the second one prepared from the more hydrophilic 4,7,10-trioxa-1,13-tridecane linker (SB/NSB = 8.0 and 11.6). Noticeably, the least efficient among all the tested NCs, the magnetite-polyDPyr-(**17a**) NC (SB/NSB = 4.2) built also on the same hydrophilic 4,7,10-trioxa-1,13-tridecaneamine linker. These results excluded this kind of PEG-like monomer internal linker for performant magnetic NCs. Additionally, both magnetite-polyDPyr(**4a**)/polyDCbz(**4b**) NCs prepared from the same monocarboxylated L-lysine-based precursor showed almost similar efficiencies (SB/NSB = 13.2 and 15.4, respectively) indicating that efficiencies are independent of the type of monomer/polymer heterocycles polyDPyr-/polyDCbz.

Sensitivity Patterns of NCs at Decreasing Concentrations of FITC-5′Labeled DNA_2 (Model Analyte). Subsequently, the above set of DNA_1-decorated NCs has also been screened in parallel to investigate the lowest sensitivity limit of detection of FITC-5′labeled DNA_2 acting as a model analyte. During these experiments, all the parameters and protocols arising from the previous study were implemented while the concentration of FITC-5′labeled DNA_2 was varied downward in the $10^{-7}-10^{-14}$ M range. Corresponding ODs and averaged NSB data (triplicate experiments) for each tested NC were reported in Figure 5. NSB data were consistently in a low 0.05−0.09 range for all tested NCs except for the magnetite-polyDPyr(**17a**) NC prepared from the hydrophilic linker 4,7,10-trioxa-1,13-tridecanediamine that averaged a high 0.11 value. Previously observed least detection efficiencies (lowest SB/NSB ratios) for this specific NC were retrieved for all tested concentrations of FITC-5′labeled DNA_2.

On the contrary, *three* magnetite-polyDPyr(**4a**), -polyDPyr-(**15a**), and -polyDPyr(**16a**) NCs from the polyDPyr-series and *four* magnetite-polyDCbz(**4b**), -polyDCbz(**8b**), -polyDCbz(**9b**), and -polyDCbz(**16b**) NCs from the polyDCbz-series were found to attain reproducible SB/NSB ratios in the 1.6−2.7 range at very low $10^{-12}-10^{-14}$ M concentrations of FITC-5′labeled DNA_2.[65] These results took a particular significance when COOH-Dynabeads similarly tested in parallel were found totally inefficient. Therefore, these novel highly sensitive magnetic NCs have an interesting potential for DNA detection at very low concentrations. Best among all the studied magnetite-polyDPyr/polyDCbz NCs was the magnetite-polyDPy(**16a**) NC that displayed the most sensitive SB/NSB ratio of 2.7 at 10^{-14} M (10 fM level) of FITC-5′labeled DNA_2.[65] The two other more sensitive NCs magnetite-polyDCbz(**4b**) and -polyDCbz(**8b**) were found an order less sensitive with similar SB/NSB ratios (2.0 and 1.6, respectively, at 10^{-13} M). Importantly, these low-range DNA detection levels at low NSB have been achieved without using any additional passivating step (incubations with egg albumin, BSA, PEG_{1000} or Triton X surfactants, dextran) commonly used in the diagnostic field.

(65) This high-level sensitivity (10 fM level) for detection of DNA hybridization already sustains comparison with other ultrasensitive detection methodologies based on fluorescence ($6 \times 10^{-12}- 1 \times 10^{-15}$ M level),[65a−e] surface plasmon resonance (SPR, 10^{-11} M),[65f] electrochemistry ($1 \times 10^{-10}-0.1 \times 10^{-15}$ M)[65g−m] and alternative/combined means involving nanoparticles (20×10^{-15} and 0.5×10^{-18} M).[65n,o] (a) Wang, G.; Yuan, J.; Matsumoto, K.; Hu, Z. *Anal. Biochem.* **2001**, *299*, 169−172. (b) Epstein, J. R.; Lee, M.; Walt, D. R. *Anal. Chem.* **2002**, *74*, 1836−1840. (c) Ali Mehnaaz, F.; Kirby, R.; Goodey, A. P.; Rodriguez, M. D.; Ellington, A. D.; Neikirk, D. P.; McDevitt, J. T. *Anal. Chem.* **2003**, *75*, 4732−4739. (d) Nie, L.; Tang, J.; Guo, H.; Chen, H.; Xiao, P.; He, N. *Anal. Sci.* **2004**, *20*, 461−463. (e) Li, H.; Rothberg, L. J. *Anal. Chem.* **2004**, *76*, 5414−5417. (f) He, L.; Musick, M. D.; Nicewarner, S. R.; Salinas, F. G.; Benkovic, S. J.; Natan, M. J.; Keating, C. D. *J. Am. Chem. Soc.* **2000**, *122*, 9071−9077. (g) Korri-Youssoufi, H.; Garnier, F.; Srivastava, P.; Godillot, P.; Yassar, A. *J. Am. Chem. Soc.* **1997**, *119*, 7388−7389. (h) Zhang, Y.; Kim, H.-H.; Heller, A. *Anal. Chem.* **2003**, *75*, 3267−3269. (i) Wang, J.; Liu, G.; Zhu, Q. *Anal. Chem.* **2003**, *75*, 6218−6222. (j) Park, N.; Hahn, J. H. *Anal. Chem.* **2004**, *76*, 900−906. (k) Hernandez-Santos, D.; Diaz-Gonzalez, M.; Gonzalez-Garcia, M. B.; Costa-Garcia, A. *Anal. Chem.* **2004**, *76*, 6887−6893. (l) Hwang, S.; Kim, E.; Kwak, J. *Anal. Chem.* **2005**, *77*, 579−584. (m) Liu, J.; Tian, S.; Tiefenauer, L.; Nielsen, P. E.; Knoll, W. *Anal. Chem.* ACS ASAP (AN **2005**:267048). (n) Cao, Y. C.; Jin, R.; Mirkin C. A. *Science* **2002**, *297*, 1536−1540. (o) Nam, J.-M.; Stoeva Savka, I.; Mirkin C. A. *J. Am. Chem. Soc.* **2004**, *126*, 5932−5933.

Conclusions

Novel oxidatively polymerizable mono- and dicarboxylated DPyr- and DCbz-monomers have been chemically designed and readily synthesized using a general and versatile route (C_2-symmetrization of NH_2-/COOH-amino acid-related building blocks). Their oxidative polymerization onto magnetite nanoparticles has been achieved using oxidants specific of monomer heterocyclic chemical type. Resulting magnetically responsive sheetlike magnetite-DPyr/-DCbz nanocomposites (20−40 nm size) have been fully characterized using a range of analytical and spectroscopic techniques. They have been shown unambiguously to possess a core−shell morphology. COOH functionalities that have been introduced by the polymeric shell allowed these NCs to be covalently modified by an aminated 20-*mer* DNA sequence (capture probe). Resulting DNA-functionalized NCs have been screened for improved properties regarding DNA hybridizations occurring onto NC surfaces using a blue-color emitting HRP-based enzymatic signal amplifying system. Observed SB/NSB ratios for the whole set of prepared NCs compared well or were even better than those of standard commercially available COOH-Dynabeads parallely treated under similar conditions. The type of monomer heterocycles Pyr or Cbz did not alter drastically the global efficiency of magnetic nanocomposites. On the contrary, the chemical type of linkers had significant effects in DNA hybridizations. Another unique capability of our approach to prepare these novel magnetically responsive magnetite-polyDPyr/-polyDCbz NCs lies in the potential combinatorial engineering of polymeric shells of NCs for optimization to a given application. The corresponding results dealing with combinatorially fabricated magnetic NCs will be reported soon in separate publications.

Acknowledgment. This work has been funded under both V^{th}/VI^{th} Framework European CHEMAG (n° GRD2-2000-30122) and NACBO (n° NMP3-2004-500802-2) projects. The authors thank Profs. Shlomo Margel for his scientific assistance in TGA analyses, Drs. Yudith and Tova Tamari for acquiring TEM and HRTEM microphotographs, and Mr. Ishai Bruckental (Department of Physics, Bar-Ilan University) for his help for magnetization measurements.

Supporting Information Available: Typical synthetic procedures, analytical and spectral characterization data of selected oxidizable DPyr-/DCbz-monomers, FT-IR spectra of selected magnetite-NCs, low- and high-resolution TEM and HR-TEM microphotographs with elemental EDAX analyses and the Mössbauer spectrum of magnetite-polyDCbz(**18b**) nanocomposite, TGA and C,H,N-elemental analyses (TGA curves and comparative table), a table of absolute magnetizations and coercivity values of NCs. This material is available free of charge via the Internet at http://pubs.acs.org.

JA050285L